

Analysis and Correlation of Internal Tumor and External Mark Motion for IGRT

Mary McLaughlin², Huanmei Wu^{1,2}, Malika Mahoui²,

¹Purdue School of Engineering and Technology

²Indiana University School of Informatics

Indiana University Purdue University Indianapolis

Indianapolis, IN 46202

Abstract: Excessive sampling images pose the risk of radiation poisoning for patients in image guided radiation treatment (IGRT). Thus, treatment methods based on external marker position (which is radiation free for sampling images) have been developed. The challenge is how to correlate external marker motion with internal tumor motion. Our research is trying to address this issue through retrospective analysis and knowledge discovery for the correlation between the external marker and internal tumor positions acquired simultaneously during treatment. A new dynamic procedure has been proposed for data processing. The normalized data was disseminated into piecewise line segments. Statistical analysis and correlation discovery, such as aggregates and histogram, were calculated based on the piecewise linear representation. The analytical results show that there is strong correlation between external and internal tumor motion. The correlation and analytical results presented here will be important input for prediction of internal tumor motion based on external marker position.

1. Introduction

With advanced technologies for high-throughput data production, medical information has been increasing exponentially in recent years. Managing, analyzing and simulating complex medical information is of great significance for medical decision-making and better patient care. This paper introduces our research effort in applying advanced statistical analysis over dynamic time series data from real-time image guided radiation treatment.

Radiation therapy is a treatment modality directed toward local control of cancer. The primary goal of radiation therapy is to ensure precise radiation delivery to kill tumor cells and minimize radiation dose to surrounding healthy tissues and critical structures. However, the quality of radiation treatment is degraded by respiratory motion^[1, 13, 14]. As patients inhale and exhale, tumors in lungs and abdominal regions move correspondingly. Direct localization of the tumor mass in real-time is often difficult. Various surrogates are then used to derive the tumor position

during the treatment, including *internal* and *external surrogates*^[1]. Internal surrogates are implanted fiducial markers inside or near the tumor. The internal tumor motion can be derived by locating the internal surrogates using fluoroscopic tracking. The precision is satisfactory. However, fluoroscopic tracking requires radiation dose for imaging. Thus, imaging dose is a primary concern for internal surrogates. External surrogates, such as markers, are placed on the surface of the patient's abdomen. External markers are radiation free. The weakness is the uncertainty in correlation between external surrogates and internal tumor position.

The aim of this research project is to find meaningful moving correlation between the internal tumor motion with external marker motion of cancer patients under the condition of free breathing during treatment. This correlation analysis can be used for further research of motion characterization and motion prediction, which are important both for pre-treatment planning and for online monitoring.

The rest of the paper will be organized as follows: Section 2 introduces the related work in the field. Section 3 presents the methods. The results are presented in section 4. The last section provides a summary of the findings and directions of future work.

2. Related Work

Tumor respiratory motion is a relatively new research field. Several models have been proposed to model tumor respiratory motion. Lujan *et al.* and Seppenwoolde *et al.* describe a method of modeling a breathing pattern with a modified cosine function^[8, 15]. Neicu *et al.* have described how to capture a more detailed waveform model using a concept called the Average Tumor Trajectory^[6]. However, the cosine model does not work well when the inhale and exhale phases are asymmetrical. Both cosine and ATT models are offline algorithms and need multiple scans over raw data which can not be used for real-time prediction. Wu *et al.* has developed a finite state model to decompose the incoming tumor motion signal into line segments during real-time image guided radiation treatment^[12].

The correlation between internal tumor motion and external marker motion has not yet been adequately validated with data directly correlating tumor and diaphragm/chest wall motion, and there are known instances where it will lead to errors^[2, 4, 5, 7, 9]. Even if a correlation between tumor motion and diaphragm/chest wall motion is observed for some patients prior to treatment, we cannot assume that the same relationship will hold throughout the treatment^[7, 10]. Dynamic correlations are needed during real-time treatment which is addressed partially in this project.

3. Methods:

In this section, we present the methods we used for data processing, including preprocessing, scaling, normalization and segmentation, for statistical analysis. This was performed through several phases, which are described in detail below.

3.1 Dynamic preprocessing

Challenges to preprocessing include missing values and irregular motion. Missing data typically occur when there is an issue with the signal. Irregular motion is a result of irregularity in the breathing cycle as noted by Wu et al^[11,12]. In this study, fifty-one treatment days and 139 beams, reflective of nine patients, were initially evaluated. Missing time values were identified and replaced following the time series pattern. Missing internal and external coordinate values were estimated using linear interpolation. Outlier values were removed via nearest neighbor averaging. The method used was to take the value prior to and post the outlier, average the two numbers and substitute the average for the outlier value^[3].

All data in Figures 1(a)-1(f) are tumor motion from treatment of the same patient on the same day, either raw motion or processed motion. Figure 1(a) depicts the raw internal motion data with missing values as demonstrated by the breaks in the lines. Figure 1(b) reflects the same data as in Figure 1(a), but after the completion of linear interpolation and nearest-neighbor averaging for outlier removal. The line segments are continuous after the preprocessing. Corresponding external motion data were also preprocessed and interpolated in the same way, but not depicted in these figures.

3.2 Normalization

Figure 1(c) depicts the internal tumor- and external-motion data after preprocessing. The figure clearly demonstrates the disparity in scales between the internal and external signals obtained via different imaging modalities. A normalization process must be performed before any data analysis can be done. In order to address the scaling difference, a normalization process was initiated after the missing values were interpolated. Internal and external coordinates were scaled using the following min max normalization formula:

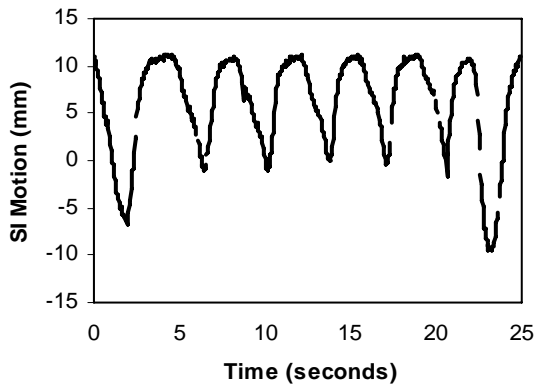
$$v' = \frac{v - \min_A}{\text{new_max}_A - \text{new_min}_A} (\text{new_max}_A - \text{new_min}_A) + \text{new_min}_A$$

where \min_A = minimum value of A, \max_A = maximum value of A. Figure 1(d) demonstrated both the internal and external marker motion after normalization, where $\text{new_max}_A = 20$ and $\text{new_min}_A = 0$ ^[3].

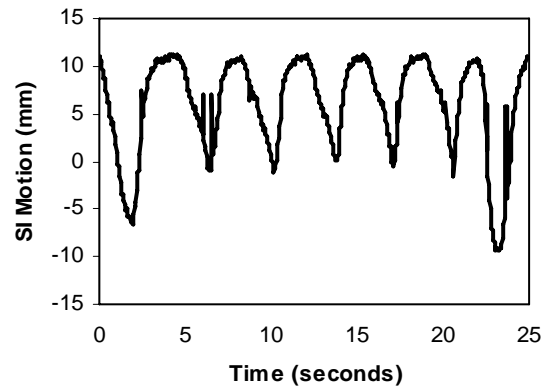
3.3 Post-normalization processing

To ensure that the data were contained within the same plane, the inverse of the normalized external coordinate plus an integer value was calculated for amplitude analysis purposes. The normalized internal and external coordinates were graphed and visually inspected. An approximation of range variance was calculated. The integer added to the normalized external coordinate was based on this approximation. Graphing and visual inspection were completed a second time. Adjustments to the integer value were made until data were contained in the same plane; this process was repeated as many times as necessary to achieve the desired results.

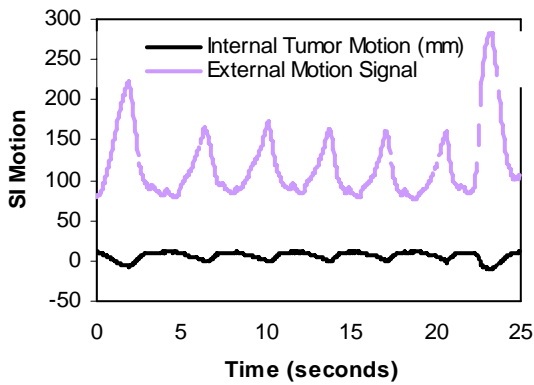
After processing and normalizing the data, both the internal tumor motion and external marker motion were decomposed into piecewise line segments based on an online implementation of a finite state model^[12]. Each line segment represents one breathing state, such as exhale (EX), inhale (IN) and end of exhale (EOE). Pre-segmented and segmented data were graphed and visually analyzed. Figure 1(e) represents the data after the post-normalization process and the data now are contained in the same plane. Figure 1(f) represents the data after segmentation.



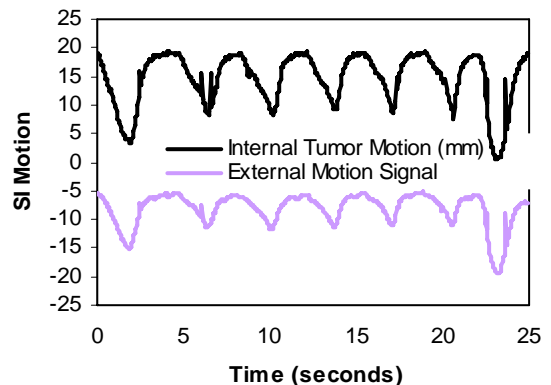
(a)



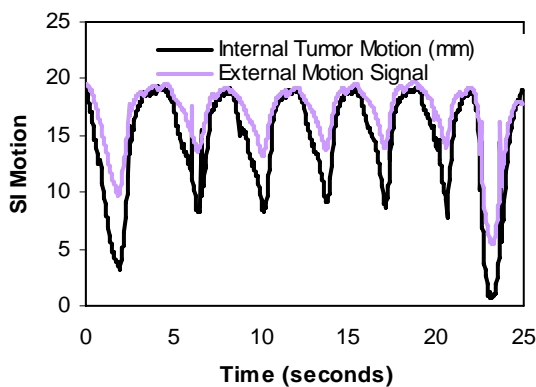
(b)



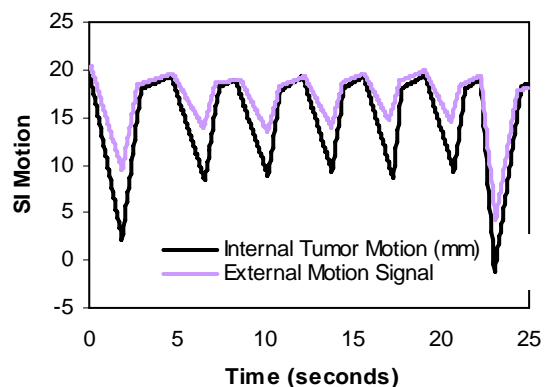
(c)



(d)



(e)



(f)

Figure 1: Motion data processing. (a) raw internal tumor motion data, (b) internal tumor motion data after interpolation, (c) internal and external motion data before scaling, (d) internal and external motion data after normalization, (e) internal and external motion data after post-normalization processing, and (f) internal and external motion data after segmentation.

3.5 Statistical analysis

There are many motion properties that can be used to discover correlation. Some properties are independent from each other, such as amplitude and frequency. Others are interrelated, such as amplitude versus starting position or duration versus starting time. We evaluated different motion parameters that we propose to use for correlation.

Twenty-eight post-segmented data files that correspond to several session beams for each patient treatment day were individually analyzed. Statistical analysis was performed on the daily motion data of each patient. Aggregated information, such as the minimum, maximum, and average of a motion fraction, or the day or the whole treatment course of the patient, was computed and compared.

In this paper, we summarize the findings of starting time difference and starting position difference between the internal and external motion coordinates. *Starting time difference* is defined as:

$$\delta t = t(\text{external}) - t(\text{internal})$$

where $t(\text{external})$ and $t(\text{internal})$ are the time instances of the beginning point of a line segment for the external and internal motion, respectively. *Starting position difference* is defined as:

$$\delta y = y(\text{external}) - y(\text{internal}).$$

where $y(\text{external})$ and $y(\text{internal})$ are the positions of the beginning point of a line segment for the external and internal motion, respectively.

4. Results and discussion

Although there are many challenges related to processing external and internal motion coordinates for lung tumor patients, the unique and dynamic normalization process demonstrated has proven effective in detecting common patterns among this set of patients. Data were aggregated for each patient treatment day and included the minimum, maximum and average for the full breathing cycle as well as each state. Histograms reflecting the difference between the internal and external coordinates for average starting time and position were developed.

A predominant pattern was identified for both the starting time and position. In 64% of the patients, the foremost pattern: $\delta t(\text{EOE}) < \delta t(\text{EX}) < \delta t(\text{IN})$ was seen for starting time difference. For starting position difference, the main pattern: $\delta y(\text{EOE}) < \delta y(\text{IN}) < \delta y(\text{EX})$ was seen 71% of the time. In addition the combination of these patterns was identified 54% of the time. Figure 2(a) and 2(b) illustrate the primary difference patterns for starting time and position.

4.1 Starting time difference

Other characteristics of the foremost starting difference pattern $\delta t(\text{EOE}) < \delta t(\text{EX}) < \delta t(\text{IN})$ include: $\delta t(\text{EOE})$ is negative at approximately 217 ms and $\delta t(\text{EX})$ is negative at approximately 69 ms. The $\delta t(\text{IN})$ can be negative or positive with values ranging from 699 to -577 ms in 96% of the cases evaluated. The cycle starting time difference was negative in 96% of all treatment days.

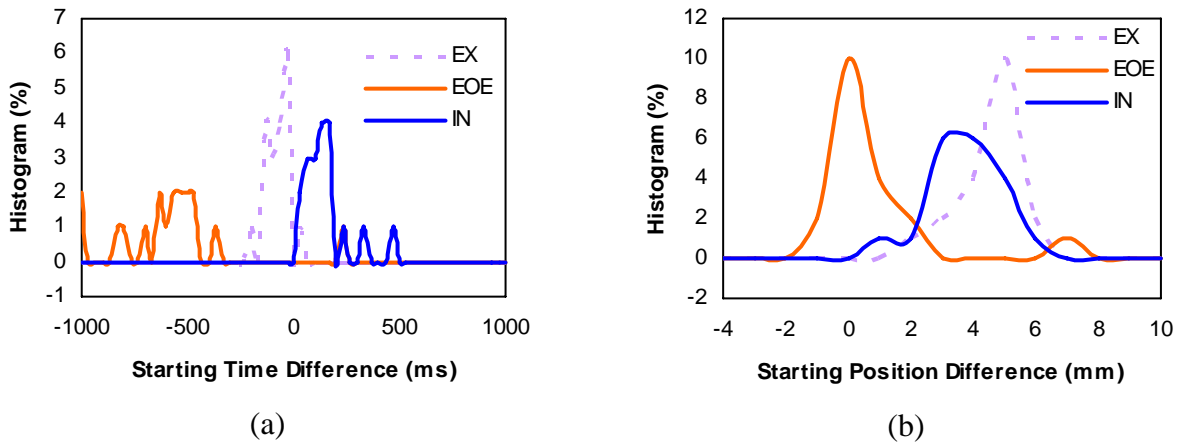


Figure 2: Statistical analytical results. (a) the histogram of starting time difference of one patient, (b) the histogram of starting position difference of the same patient.

This predominant pattern reflects that the EOE duration for the external motion is greater than that of the internal motion. The EX and IN duration for the external motion is less than that of the internal motion.

The second most frequently observed starting difference pattern was: $\delta t(\text{EX}) \sim \delta t(\text{EOE}) \sim \delta t(\text{IN})$. This was illustrated in 11% of the patient treatment days and was seen in one patient. It reflects minimal movement for all states. This patient also demonstrated a positive starting difference.

The third pattern seen in seven percent of the patient treatment days was: $\delta t(\text{EOE}) < \delta t(\text{EX}) \sim \delta t(\text{IN})$. In comparison to the predominant one, there is minimal movement during the inhale phase for this particular pattern.

4.2 Starting position difference

As with starting time difference, there were three patterns demonstrated for starting position difference as well. In the predominant pattern ($\delta y(\text{EOE}) < \delta y(\text{IN}) < \delta y(\text{EX})$) noted: (EOE) was negative at approximately -13 ms in 71% of all treatment days. The $\delta y(\text{IN})$ and $\delta y(\text{EX})$ were positive or negative values with ranges between -29 ms to 72 ms and -152 ms to 109 ms, respectively. The average movement for each of these states was: 6 ms for IN and 36ms for EX.

This primary pattern reflects that the EOE amplitude for the external motion is less than that of the internal motion. Although the ranges for EX and IN starting position values were varied, the pattern demonstrated that the external motion is greater than the internal motion.

The second most established pattern displayed was: $\delta y(\text{IN}) < \delta y(\text{EOE}) < \delta y(\text{EX})$. This was reflected in 11% of the patients, but not in just one patient as the second most frequent starting time difference pattern was. In this pattern, the IN and EOE states are in reverse order in regard to difference in movement as compared to the main pattern.

The third pattern exhibited was: $\delta y (EX) < \delta y (EOE) < \delta y (IN)$. This pattern was prevalent in seven percent of the treatment days and seen in more than one patient. In this case, the EX state movement was less than the other two states.

5. Conclusion and future work

Predominant correlation patterns between external marker motion and internal tumor motion were identified for the starting time and position utilizing preprocessing, normalization, post-processing and piecewise linear segmentation. The statistical results show that there are strong correlations. The primary pattern for starting time difference was $\delta t(EOE) < \delta t(EX) < \delta t(IN)$. For starting position difference, it was $\delta y (EOE) < \delta y (IN) < \delta y (EX)$. These patterns were seen 64% and 71% of the time, respectively. In addition a combination of these patterns was identified in 54% of the cases.

These results are promising, but further detailed correlation discovery is required. Analysis of amplitude and cycle duration differences is needed to identify if common patterns exist among these factors as well. In addition, utilizing the current work as a basis for prediction of tumor or external motion will be investigated.

Reference

1. Engelsman, M., et al., The effect of breathing and set-up errors on the cumulative dose to a lung tumor. *Radiother Oncol*, 2001. 60(1): p. 95-105
2. P Giraud, Y De Rycke, B Dubray, S Helfre, D Voican, L Guo, JC Rosenwald, K Keraudy, MHousset, E Touboul, and JM Cosset. Conformal Radiotherapy (CRT) Planning for Lung Cancer: Analysis of Intrathoracic Organ Motion During Extreme Phases of Breathing. *Int J Radiat Oncol Biol Phys*, 51(4):1081–92, 2001.
3. J Han and M Kamber, *Data Mining Concepts and Techniques*, Second Edition 2006.
4. T Iwasawa, Y Yoshiike, K Saito, S Kagei, T Gotoh, and SMatsubara. Paradoxical motion of the Hemidiaphragm in Patients with Emphysema. *J Thorac Imaging*, 15(3):191–195, 2000.
5. S Minohara, T Kanai, M Endo, K Noda, and M Kanazawa. Respiratory Gated Irradiation System for Heavy-ion Radiotherapy. *Int J Radiat Oncol Biol Phys*, 47(4):1097–1103, 2000.
6. T. Neicu, H. Shirato, Y. Seppenwoolde, and SB Jiang. Synchronized Moving Aperture Radiation Therapy (SMART): Average Tumor Trajectory for Lung Patients. *Phys. Med. Biol.*, 48(5):587–598, 2003.
7. C. Ozhasoglu and M. J. Murphy. Issues in Respiratory Motion Compensation During External-beam Radiotherapy. *Int J Radiat Oncol Biol Phys*, 52(5):1389–99, 2002. Journal Article.
8. Y Seppenwoolde, H Shirato, K Kitamura, S Shimizu, and J R Adler. Precise and Real-time Measurement of 3D Tumor Motion in Lung Due to Breathing and Heartbeat, Measured During Radiotherapy. *Int. J. Radiat. Oncol. Biol. Phys.*, 53(4):822–34, 2002.
9. CW Stevens, RF Munden, KM Forster, JF Kelly, Z Liao, G Starkschall, S Tucker, and R Komaki. Respiratory driven Lung Tumor Motion is Independent of Tumor Size, Tumor Location, and Pulmonary Function. *Int J Radiat Oncol Biol Phys*, 51(1):62–68, 2001.
10. SS Vedom, VR Kini, PJ Keall, V Ramakrishnan, H Mostafavi, and R. Mohan. Quantifying the Predictability of Diaphragm Motion During Respiration with a Noninvasive External Marker. *Medical Physics*, 30(4):505–513, 2003.
11. Huanmei Wu, Betty Salzberg, Gregory Sharp, Steve Jiang, Hiroki Shirato, and David R. Kaeli. Subsequence matching on structured time series data. In *SIGMOD Conference*, 2005.

12. Huanmei Wu, Gregory C Sharp, Betty Salzberg, David Kaeli, and Steve B Jiang. A Finite State Model for Respiratory Motion Analysis in Image Guided Radiation Therapy. *Phys. Med. Biol.*, 49(23):5357–5372, 2004.
13. Jiang, S.B., C. Pope, K.M. Al Jarrah, J.H. Kung, T. Bortfeld, and G.T. Chen, *An experimental investigation on intra-fractional organ motion effects in lung IMRT treatments*. *Phys Med Biol*, 2003. **48**(12): p. 1773-84
14. van Herk M 2004 Errors and margins in radiotherapy, *Semin. Radiat. Oncol.* 14(1) 52-64.
15. Lujan, A.E., E.W. Larsen, J.M. Balter, and R.K. Ten Haken, A method for incorporating organ motion due to breathing into 3D dose calculations. *Med Phys*, 1999. 26(5): p. 715-20.

Mary McLaughlin is a first year Ph.D. student at Indiana University School of Informatics. She has BS and MA in Dietetics and an MBA. Her research interests are focused on data management and data integration in the field of healthcare. She also is interested in data mining and prediction related to health behaviors and economics.

Dr. Huanmei Wu is an assistant professor in Purdue School of Engineering and Technology, IUPUI, joint with Indiana University School of Informatics. Dr. Wu's major research interests include database, data mining, biomedical science, medical physics (especially for image guided radiation treatment of moving tumors), and Subsequence similarity matching over time series stream data.

Dr. Malika Mahoui is currently an assistant professor in Indiana University School of informatics. Dr. Mahoui's current research interests are focused on data management and data integration in the field of bioinformatics. Her other research interests relate to the following areas: algorithmic and design issues in database systems, concurrency control and transaction processing, digital libraries, data mining and text mining, security in the web.